View metadata, citation and similar papers at core.ac.uk
brought to you by CORE
provided by Digital library of Brno University of Technology

Cross-Wire Calibration for Freehand 3D Ultrasonography: Measurement and Numerical Issues

Asterios ANAGNOSTOUDIS, Jiří JAN

Dept. of Biomedical Engineering, Brno University of Technology, Kolejní 4, 612 00 Brno, Czech Republic

asterios@feec.vutbr.cz, jan@feec.vutbr.cz

Abstract. *3D freehand ultrasound is an imaging technique, which is gradually finding clinical applications. A position sensor is attached to a conventional ultrasound probe, so that B-scans are acquired along with their relative locations. This allows the B-scans to be inserted into a 3D regular voxel array, which can then be visualized using arbitrary-plane slicing, and volume or surface rendering. A key requirement for correct reconstruction is the calibration: determining the position and orientation of the B-scans with respect to the position sensor's receiver. Following calibration, interpolation in the set of irregularly spaced B-scans is required to reconstruct a regular-voxel array. This text describes a freehand measurement of 2D ultrasonic data, an approach to the calibration problem and several numerical issues concerned with the calibration and reconstruction.*

Keywords

3D freehand ultrasonography, cross-wire calibration phantom, 3D freehand ultrasound calibration.

1. Introduction

Conventional 2D ultrasonic imaging uses a hand-held probe, which transmits ultrasound pulses into the body and receives the echoes. The magnitude and timing of the echoes are used to create a 2D grey-level image (B-scan) of a cross-section of the body in the scan plane. 3D ultrasonography extends this concept so that volumes of intensity data are created from pulse-echo information.

The 3D freehand imaging technique can be subdivided into three stages: scanning, reconstruction, and visualizations. A common ultrasonic probe is freely moved over the patient's body, so that the acquired B-scans have arbitrary relative locations and may overlap each other.

Electromagnetic or optical position-sensing devices, consisting of an electromagnetic transmitter and a receiver, or optical cameras and LED markers, respectively, are used to determine the position and orientation of the acquired B-scans. Before scanning, the receiver (or LED markers) is attached to the probe and the transmitter (or couple of optical cameras) is placed in a fixed position. The acquired B-scans and their relative positions are consequently used to fill a regular voxel array, which can then be visualized [6] using arbitrary-plane slicing, multi-planar reformatting, volume rendering or surface rendering.

The position-sensing devices, used to determine the position and orientation of the acquired B-scans, can be optical, electromagnetic or mechanical. The optical devices are supposed to be more accurate allowing six degrees of freedom for the probe motion, but at the same time they are more expensive than the others and require full time optical contact between the camera and the LED markers. This is a quite difficult task when for example the 3D ultrasound is used as a tool for navigation during operation. The mechanical devices allow only three degrees of freedom, which is quite limiting in a freehand measurement since the range of possible probe movements is significantly decreased. The electromagnetic devices are less accurate than optical, since they are working on the base of transmitted and received electromagnetic waves, which can be influenced by surrounding electrically conducting devices and therefore lead to slightly inaccurate measurements. However, this error is not of such a degree that wouldn't allow them to be used for reconstruction of 3D ultrasound data, as seen from the large amount of publications on 3D ultrasound calibration where the correct use of electromagnetic devices is described, leaving no doubt for their practical usability in this specific area. At the same time they are quite cheaper than the optical ones.

We used the electromagnetic MiniBIRD position-sensing device (Ascension Technology Corporation) that allows 6 degrees of freedom. The transmitter transmits a pulsed DC magnetic field that is measured by the receiver. From the field characteristics, the MiniBIRD computes the position and orientation of the receiver. The sensor is capable of making up to 120 measurements/sec when it is located within 76 cm from the transmitter. The manufacturers claim a static resolution of 0.5 mm in change of position and 0.1˚ in change of orientation. The positional accuracy is 1.8 mm and the orientation accuracy 0.5˚. The pulsed DC technology employed by the MiniBIRD has minimal sensitivity to metal: five times less susceptible to distortion caused by nearby metal than AC technology. Therefore, medical grade stainless steel does not affect the tracker.

2. Reconstruction

Fig. 1 shows the four coordinate systems (c.s.) used for reconstruction. ***P*** is the c.s. of the B-scan plane, placed at the upper left corner of the B-scan. The *y*-axis is in the beam direction, the *x*-axis is in the lateral direction and the *z*-axis in the elevation direction, out of the B-scan plane. ***R*** is the c.s. of the moving receiver and ***T*** the c.s. of the fixed transmitter. The reconstruction volume, to be filled by the set of acquired B-scans, takes the form of a 3D matrix of voxels. ***C*** is its c.s. placed at its corner.

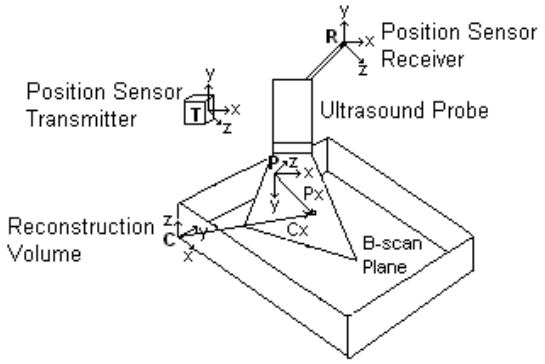

Fig. 1. The four coordinate systems used during the reconstruction process.

For every pixel in every B-scan we have to locate its nearest corresponding voxel in the reconstruction volume. The vector ${}^{P}\boldsymbol{x}$ shows the location of each pixel in the B-scan, i.e. the distance of a pixel from ***P***. Each B-scan pixel's location, is transformed to ***R***, then to ***T*** and finally to ***C***. The overall transformation, which can be expressed as a multiplication of homogeneous transformation matrices, results in the vector ${}^{C}\boldsymbol{x}$ that represents the pixel's location in the coordinate system ***C***, i.e. a distance of each voxel from ***C***:

$$ {}^{C}\mathbf{x} = {}^{C}\mathbf{T}_{T}\ {}^{T}\mathbf{T}_{R}\ {}^{R}\mathbf{T}_{P}\ {}^{P}\mathbf{x}, \tag{1} $$

$$ {}^{P}\mathbf{x} = \begin{pmatrix} s_x u & s_y v & 0 & 1 \end{pmatrix}^{T} \tag{2} $$

where ${}^{J}\mathbf{T}_{I}$ is the transformation from the c.s. ***I*** to the c.s. ***J***, *u* and *v* are the column and row indices of the B-scan pixels, and s_x and s_y are scale factors of pixels [mm/pixel]. The row and column indices of the cross-wire intersection point in the B-scan image can be detected either manually or automatically by a feature detection algorithm. Since the detectable point in the B-scan covers an area of several pixels, we can consider the middle pixel of the area as the one corresponding to the calibration point.

A transformation between two coordinate systems has six degrees of freedom: three rotations (α, β, γ) and three translations (***x***, ***y***, ***z***). The rotation between two coordinate systems is effected by first rotating e.g. through α around the *x*-axis, then through β around the *y*-axis, and finally through γ around the *z*-axis. The fixed rotation axes are aligned with the first coordinate system. Using this convention, the homogeneous matrix describing the transformation takes the following form:

$$ {}^{J}T_{I}(x,z,y,\alpha,\beta,\gamma) = \begin{pmatrix} \cos\alpha\cos\beta & \cos\alpha\sin\beta\sin\gamma - \sin\alpha\cos\gamma & \cos\alpha\sin\beta\cos\gamma + \sin\alpha\sin\gamma & x \\ \sin\alpha\cos\beta & \sin\alpha\sin\beta\sin\gamma + \cos\alpha\cos\gamma & \sin\alpha\sin\beta\cos\gamma - \cos\alpha\sin\gamma & y \\ -\sin\beta & \cos\beta\sin\gamma & \cos\beta\cos\gamma & z \\ 0 & 0 & 0 & 1 \end{pmatrix} \tag{3} $$

From the MiniBIRD readings we derive the transformation matrix ${}^{T}\mathbf{T}_{R}$, giving the position and orientation of ***R*** with respect to ***T***. The 6 parameters (rotations and translations) of ${}^{R}\mathbf{T}_{P}$, the 6 parameters of ${}^{C}\mathbf{T}_{T}$ and the 2 scale factors s_x and s_y, need to be determined by calibration.

3. Calibration

Calibration is performed by scanning a phantom of known geometric structure and dimensions. We can write equations similar to (1) using knowledge of the phantom geometry and the position sensor measurements. Solving the equations we determine the calibration parameters. Several calibration methods exist. Some rely on point targets such as small spheres [3] or intersection of thin wires [1]. Others detect plane targets as the bottom of a water bath [1], membranes [4, 9] or planes constructed from parallel wires [5, 8].

3.1 Cross-Wire Phantom

It is the most commonly used phantom, because of the easiness to construct and scan it, and since it gives precise enough calibration results compared to other techniques [1].

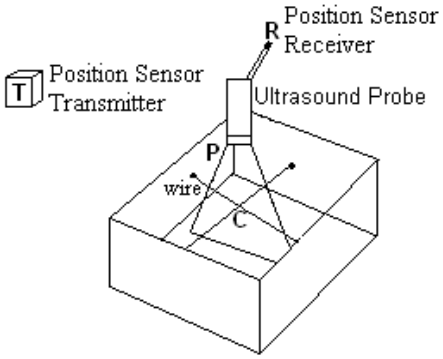

Fig. 2. Cross-wire calibration phantom.

It consists of two very thin intersecting wires mounted on a wooden frame and inserted in water bath. We used nylon wires of 0.3 mm diameter. The transmitter was placed at some fixed location nearby (Fig. 2). The location where the wires cross has been repeatedly scanned from different directions. In each B-scan, a detectable cross-point appears. For calibration purposes, the origin of ***C*** is not regarded coincident with the corner of the reconstruction volume but with the wire intersection. This makes the distance from the origin of ***C*** to the cross-wire point, i.e. the *x*, *y* and *z* components of the ${}^{C}\mathbf{x}$ vector, equal to zero. According to (1), the B-scan pixel at the centre of the cross should then satisfy the equation

$$\begin{pmatrix}0 & 0 & 0 & 1\end{pmatrix}^T = {}^C\mathbf{T}_T\ {}^T\mathbf{T}_R\ {}^R\mathbf{T}_P \begin{pmatrix}s_x u & s_y v & 0 & 1\end{pmatrix}^T . \quad (4)$$

The first three rows of (4) give the three equations involving the measurements ${}^T\mathbf{T}_R$, u and v, and the unknowns ${}^R\mathbf{T}_P$, ${}^C\mathbf{T}_T$, s_x and s_y. If there are m B-scans, then the respective equations can be stacked together to produce a system of non-linear homogeneous equations of the size $3m$. We have measured 30 B-scans and therefore obtained a system of 90 equations:

$$\mathbf{0} = \mathbf{f}(\boldsymbol{\theta}, \boldsymbol{\varphi}) \quad (5)$$

where $\boldsymbol{\theta}$ are the known quantities ${}^T\mathbf{T}_R$, u and v, while $\boldsymbol{\varphi}$ are the unknowns ${}^R\mathbf{T}_P$, ${}^C\mathbf{T}_T$, s_x and s_y. Therefore, $\boldsymbol{\varphi}$ is a 14-element vector, composed of the 6 parameters of ${}^R\mathbf{T}_P$, the 6 parameters of ${}^C\mathbf{T}_T$ and the two scale factors. However, the coordinate system $\boldsymbol{C}$ can be of any orientation and still satisfy (4). This means that the three orientation angles of ${}^C\mathbf{T}_T$ can be set to zero in (5) and only 11-elements of $\boldsymbol{\varphi}$ are to be found. Thus, a system of 90 equations, with 11 unknowns had to be solved. This over-determined system has been solved by the Levenberg-Marquardt algorithm in frame of the Matlab's optimization toolbox [2]. Another possibility is to use the Gauss-Newton algorithm in frame of the Matlab's optimization toolbox [2].

3.2 Solving the System of Non-Linear Equations

The algorithm used for the solution of the system is the Levenberg-Marquardt algorithm as a part of the Matlab's Optimization Toolbox [2]. The algorithm is iterative and tries to find the closest possible solution possibly avoiding local extrema. It needs an initial guess of the solution to the problem (a starting point). This guess could be any rough estimate of the true solution, but the closer it is to the true solution, the quicker the convergence. The initial estimate in a probe calibration can be found from a physical measurement of the translation with a ruler, and approximate knowledge about sensor orientation relative to the ultrasound image plane.

The Levenberg-Marquardt algorithm works in the following way

$$\begin{aligned}&\mathbf{0} = \mathbf{f}(\boldsymbol{\theta}, \boldsymbol{\varphi}) \approx \mathbf{f}(\boldsymbol{\theta}, \boldsymbol{\varphi}_\mathbf{j}) + \frac{\partial \mathbf{f}(\boldsymbol{\theta}, \boldsymbol{\varphi}_\mathbf{j})}{\partial \boldsymbol{\varphi}} \left(\boldsymbol{\varphi} - \boldsymbol{\varphi}_\mathbf{j}\right) \Rightarrow \\ &\Delta\mathbf{f} = \mathbf{J}\left(\boldsymbol{\varphi} - \boldsymbol{\varphi}_\mathbf{j}\right) = \mathbf{J}\,\Delta\boldsymbol{\varphi}\end{aligned} \quad (6)$$

where $\Delta\mathbf{f}$ is the error vector $-\mathbf{f}(\boldsymbol{\theta}, \boldsymbol{\varphi}_\mathbf{j})$ and $\mathbf{J}$ is the gradient matrix $\partial\mathbf{f}(\boldsymbol{\theta}, \boldsymbol{\varphi}_\mathbf{j})/\partial\boldsymbol{\varphi}$, also known as the Jacobian. The Levenberg-Marquardt algorithm produces the updated parameter vector values $\boldsymbol{\varphi}_{\mathbf{j+1}}$:

$$\boldsymbol{\varphi}_{\mathbf{j+1}} = \boldsymbol{\varphi}_\mathbf{j} + \left(\mathbf{J}^T\,\mathbf{J} + \varepsilon\ \mathbf{I}\right)^{-1} \mathbf{J}^T\,\Delta\boldsymbol{\varphi} \quad (7)$$

where ε is a damping term chosen at each step to stabilize the convergence. This method becomes the standard iterative least squares algorithm for $\varepsilon = 0$. At each step, $\Delta\mathbf{f}$ and $\mathbf{J}$ are evaluated at the current estimate $\boldsymbol{\varphi}_\mathbf{j}$. This process is iterated until the corrections $\Delta\boldsymbol{\varphi}$ are sufficiently small.

In case the input data (number of B-scans and corresponding probe positions and angles) are numerous and differ from each other (covering all possible probe angles and positions), the algorithms converge quickly to a precise solution. Otherwise the result may not be accurate enough.

It is a future task to find the proper extent of input data needed for robust and accurate calibration. In our case, because of lack of a-priori knowledge, we have measured just 30 B-scans. It turned out, that the algorithm could not manage to compute the final exact solution but just a rough estimate that doesn't allow us to perform a reconstruction, precise enough for medical-diagnostic purposes. In a future measurement, we are planning to measure at least 300 B-scans and compare the solutions obtained from a successively decreasing number of equations in order to estimate the minimum needed for a precise solution.

3.2.1 A Comment on Mirror Solutions

Several distinct angles and scales produce the same calibration. We call these "mirror solutions". In order to compare solutions, we have to adopt a canonical form for the angles and scales. This requires that

- s_x and s_y are positive,
- α and γ are in the range $\pm\pi$,
- β is in the range $\pm\pi/2$.

The procedure [1] for enforcing these constraints includes:

- Limit all the angles to the range $\pm\pi$ by adding or subtracting $k2\pi$.
- If β is outside of $\pm\pi/2$, add or subtract π to correct it, and add π to both α and γ.
- If $s_y < 0$, change γ to $\gamma+\pi$ and s_y to $-s_y$.
- If $s_x < 0$, change α to $\alpha+\pi$, β to $-\beta$, and s_x to $-s_x$.
- Check that α and γ are still within $\pm\pi$. If not, repeat the step 1.

3.3 Some Numerical Results

For all attempts, the software used was Matlab's Optimization Toolbox. The algorithm used mostly was the Levenberg-Marquardt algorithm. The Gauss-Newton algorithm yielded the same results. The system $\mathbf{f}$ could look like the following example:

$$\begin{aligned}f_1 &= 0.422\cos\alpha\cos\beta\, s_x u + 0.712\sin\alpha\cos\beta\, s_x u + 0.560\sin\beta\cdots \\ f_2 &= 0.470\cos\alpha\cos\beta\, s_x u - 0.701\sin\alpha\cos\beta\, s_x u - 0.470\sin\beta\cdots \\ &\vdots \\ f_{90} &= 0.774\cos\alpha\cos\beta\, s_x u + 0.036\sin\alpha\cos\beta\, s_x u - 0.774\sin\beta\cdots\end{aligned} \quad (8)$$

In every attempt we choose a starting point. The algorithm starts from that point and iteratively searches for the closest solution checking at each step the residual R, which is the sum of all squared function values:

$$R = \sum_{1}^{90} f_i^2 . \quad (9)$$

For understanding of the following results **f** will be the set of all function values: $\mathbf{f} = \{f_1, f_2, \ldots, f_{90}\}$.

1st attempt: Starting point x = ($\alpha,\beta,\gamma,s_x, s_y, {}^rx_p, {}^ry_p, {}^rz_p, {}^cx_t, {}^cy_t, {}^cz_t$) = (0, 0, 0, 0, 0, 0, 0, 0, 0, 0, 0)					
	α[°]	β[°]	γ[°]	s_x[mm]	s_y[mm]
B[1]	-90.6018	-0.2578	-27.2843	-0.1475	-0.1504
A[2]	89.3982	0.2578	27.2843	0.1475	0.1504
2nd attempt: Starting point x = (1, 1, 1, 1, 1, 1, 1, 1, 1, 1, 1)					
	α[°]	β[°]	γ[°]	s_x[mm]	s_y[mm]
B[1]	89.3982	0.2578	27.2843	0.1475	0.1504
A[2]	-	-	-	-	-
3rd attempt: Starting point x = (pi, pi/2, pi/4, 0.1, 0.15, 5, 45, 89, 60, 15, 300)					
	α[°]	β[°]	γ[°]	s_x[mm]	s_y[mm]
B[1]	89.3982	0.2578	27.2843	0.1475	0.1504
A[2]	-	-	-	-	-
4h attempt: Staring point x = (152, 48, 15, 0.1, 0.15, 5, 45, 89, 60, 15, 300)					
	α[°]	β[°]	γ[°]	s_x[mm]	s_y[mm]
B[1]	8189.4	3059.7	1107.3	0.1475	-0.1504
A[2]	89.4	-0.3	27.3	0.1475	0.1504
5th attempt: Starting point x = (-12, 256, -58, 2, 8, 12, 25, 86, 52, 598, 4)					
	α[°]	β[°]	γ[°]	s_x[mm]	s_y[mm
B[1]	810.5978	$1.458*10^4$	$-3.3927*10^3$	0.1475	0.1504
A[2]	89.4022	0	27.27	0.1475	0.1504
Average Rotations and Scale Factors (from all 5 attempts)					
α[°]		β[°]	γ[°]	s_x[mm]	s_y[mm]
89.3994		0.0947	27.2846	0.1475	0.1504

Tab. 1. Estimated and average rotations and scaling factors from the system of 11 unknowns for five different starting points. B[1]: Before and A[2]: After correction.

3.4 Scale Factor Computation

The scale factors used for the formation of the calibration matrix ${}^R\mathbf{T}_P$ were estimated by solving the system of non-linear equations with the Levenberg-Marquardt method. The scale factors can be also calculated directly instead of being estimated, using the ultrasound system parameters, and then compared to the estimated ones. We can also use those computed scale factors as constants during the solution of the system of non-linear equations thus decreasing its complexity.

The ultrasound system used (System FiVe, GE Vingmed Ultrasound) measures 1D radio-frequency (rf) ultrasound signals (beams) and saves them into frames that correspond to B-scans. Therefore, each frame consists of a number of beams (171 in our case), each having a concrete number of samples (712 in our case). Those frames are then converted from polar to Cartesian coordinates and the resulted image is the standard sector image (B-can), which consists of a number of pixels (712x867 in our case).

The following parameters are the same for all 5 attempts					
Estimated Distances [mm]					
${}^rx_p$	${}^ry_p$	${}^rz_p$	${}^cx_t$	${}^cy_t$	${}^cz_t$
-36.3443	-63.9183	204.1093	-83.7324	22.548	314.2971
***Residual* = 26.3621**		***Max(f)* = 1.4596**		***Min(f)* = -1.6505**	
Other parameters					
***Average(f)* = $-4.0530*10^{-8}$ to $3.3814*10^{-8}$ (different for different attempts)**		***# of Iterations*: 41 to 65 (depends on the start point)**		***Time*: 1.688 to 2.906 sec on PC with Pentium 4 2.66GHz, 1GB RAM**	

Tab. 2. Estimated distances from the system of 11 unknowns, and statistic values.

Knowing the number of samples *s* in each beam *b* and the constant depth increment *di* between the samples we can calculate the depth of measurement *d* (Fig. 3). Dividing this with the number of column pixels *cp* in the final B-scan gives the scale factor s_y. Concretely, for $di = 1.5428 \cdot 10^{-1}$ mm, $s = 712$, and $cp = 712$, follows $d = 109.6931$ mm and $s_y = 0.15407$.

Knowing the number of ultrasound beams *b* and the constant angle increment *ai* between them we can calculate the total opening angle *a* of the B-scan. From this angle *a* and the depth *d* we can then calculate the opening width *w* of the B-scan in *x*-direction as shown in Fig. 3. Dividing *w* by the number of pixels in each row *rp* gives the scale factor s_x. Concretely, for $ai = 0.0077$ rad or 0.4412° and $b = 171$, follows $a = 1.309$ rad or 75.0002° and $w = 133.5626$ mm. For $rp = 867$, follows $s_x = 0.1541$.

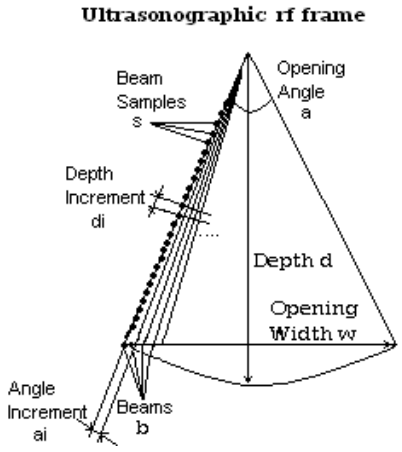

Fig. 3. An ultrasound rf frame.

3.5 Solving the System of Non-Linear Equations using the Computed Scale Factors

When the scale factors are considered to be known and equal to the computed ones, the system of 90 non-linear equations has now 11–3 = 9 unknowns. Following

the same procedure for elimination of the mirror solutions as in section 3.2.1, and for the same 5 starting points as in section 3.3, the average set of values depicted in Tab. 3 has been obtained.

Average Rotations and Scale Factors					
α[°]	β[°]	γ[°]	s_x[mm]	s_y[mm]	
89.7616	0.0334	27.771	0.155	0.1542	
The following parameters are the same for all attempts					
Estimated Distances [mm]					
${}^{r}x_p$	${}^{r}y_p$	${}^{r}z_p$	${}^{c}x_t$	${}^{c}y_t$	${}^{c}z_t$
-37.8414	-67.042	204.6028	-83.6182	22.1456	310.7523
Residual= 47.2149		Max(*f*) = 1.9674		Min(*f*) = -1.6788	
Other parameters					
Average(*f*) = -9.6347*10^{-8} to 4.9978*10^{-8} (different for diff. attempts)		# of Iterations: 1090 to 7207 (depending on the starting point)		Time: 37 to 238 sec on PC with Pentium 4, 2.66 GHz, 1 GB RAM	

Tab. 3. Estimated average rotations and scale factors and estimated distances from the system of 9 unknowns.

The difference between the average solution values of Tab. 1 and Tab. 3 is very small. However, the residual value of Tab. 3 is the double of that in Tab. 2 and the maximum, minimum, and average **f** and the number of iterations is greater. Therefore, the first approach may be considered better and the values of table 1 and 2 have been used for the construction of the final calibration matrix.

3.6 Calibration Matrix and Reconstruction

The estimated values of Tab. 1 are considered basically correct (although not quite precise because of lack of adequate input data) and therefore, the transformation matrices ${}^{R}\mathbf{T}_P$ and ${}^{C}\mathbf{T}_T$ can be computed, as well as the corresponding voxel for each B-scan pixel. This procedure is time consuming because it has to be done: 712 x 867 (# of pixels) x 30 (# of B-scans) = 18.519120 x 10^6 times.

Since the position of the B-scans is known, some interpolation techniques can be applied between the scans to reconstruct a 3D volume. The simpler the interpolation technique, the quicker the result but the less precise is the reconstructed volume. Simple interpolation techniques used in 3D ultrasound volume reconstruction are the voxel nearest neighbor [7] and the pixel nearest neighbor interpolation [7]. More complex and time consuming but also more precise technique is the radial basis function interpolation [7]; intermediate (with respect to time requirements and precision) techniques are those based on distance weighting. In the future work it is intended to apply such techniques to the data.

4. Discussion

In section 3.4, an approach for the computation of the scaling factors is presented. The computed scale factor s_y has been found equal to 0.15407, while the estimated one is 0.1504. The difference between the computed and the estimated s_y is 0.0037 yielding a quite good estimation even if the number of input data was very small as mentioned previously. Consider that the depth of measurement i.e. the y-dimension (height) of the frame is found 109.7 mm using the computed scale factor, and 107.0848 mm using the estimated scale factor, thus with a difference of just 2.6152 mm. Similarly, the computed scaling factor s_x equals to 0.1541, while the estimated one equals to 0.147 and therefore, the difference is 0.0071. This difference cannot be considered anymore negligible because, if we compute the x-dimension (width) of the frame using the estimated s_x we find it equal to 127.449 mm, and using the computed one, is equal to 133.5626 mm. The difference is noticeable now 6.1136 mm.

Measuring a greater amount of input data (B-scans and corresponding probe positions and orientations), while covering all possible probe positions and orientations, we will be able to create a highly over-determined system of non-linear equations where each equation will vary from the others. Such a system will be quickly and precisely solved by an iterative optimization algorithm and more precise calibration results will be provided.

In section 3.5, the computed scale factors have been inserted in the system of non-linear equations, thus reducing the number of unknowns to 9. It was expected that the algorithm will now converge faster and that the resulting solution would be more precise, i.e. the residual would be smaller. Unfortunately the opposite happened. The residual has doubled and the number of iterations increased to several thousands. The reason of this behavior is so far unknown and becomes a matter of further investigation.

5. Conclusions

The cross-wire calibration technique is the most commonly used technique, since it is easy to construct and scan such a phantom and mainly because it is supposed to give precise calibration results [1]. However, it is a time consuming method since a great number of B-scans has to be measured for the algorithm to converge quickly and accurately, and the cross-wire point in each B-scan has to be detected manually. A simple automatic feature detection algorithm would probably fail to recognize them because of speckle noise, reflection from the bottom of the water tank and other artifacts. An algorithm suitable for solving the over-determined calibration system was found to be the iterative Levenberg-Marquardt algorithm.

Acknowledgments

The described research was financially supported by the Czech Grant Agency under grant No. 102/02/0890, partly also by the Czech Ministry of Education No. MSM 0021630513 and the research program MSM 262200011.

References

[1] PRAGER, R., ROHLING, R., GEE, A., BERMAN, L. Rapid calibration for 3D freehand ultrasound. *Ultrasound in Medicine and Biology*, 1998, vol. 24, no. 6, p. 855 - 869.

[2] Optimization Toolbox. For Use with MATLAB. User's Guide Version 2. The Mathworks, 2002.

[3] AMIN, D., KANADE, T., JARAMAZ, B., DiGIOIA, A., NIKOU, K., LaBARCA, R., MOODY, J. Calibration method for determining the physical location of the ultrasound image plane. In *Proceedings Medical Image Computing and Computer-Assisted Intervention 2001*, *Lecture Notes in Computer Science*. 2001, vol. 2208, p. 940 - 947.

[4] LANGØ, T., LINDSETH, F., KASPERSEN J., GRØNNINGSÆTER A. Novel probe calibration methods for 3D freehand ultrasound. Submitted to *Computer Aided Surgery*, 2000.

[5] LEOTTA, D. An efficient calibration method for freehand 3D ultrasound imaging system. *Ultrasound in Medicine and Biology*, 2004, vol. 30, no. 7, p. 999 - 1008.

[6] FENSTER, A., DOWNEY, D. Three-dimensional ultrasound imaging and its use in quantifying organ and pathology volumes. *Analytical and Bioanalytical Chemistry,* 2003, vol. 377, no. 6, p. 982 - 989.

[7] ROHLING, R., GEE, A., BERMAN, L., TREECE, G. Radial basis function interpolation for freehand 3D ultrasound. In *Proceedings of 16th International Conference Information Processing in Medical Imaging,* Visegrad (Hungary), 1999.

[8] BOUCHET, L., MEEKS, S., GOODCHILD, G., BOVA, F., BUATTI, J., FRIEDMAN, W. Calibration of three-dimensional ultrasound images for image-guided radiation therapy. *Physics in Medicine and Biology*, 2001, vol. 46, p. 559 – 577.

[9] SATO, Y., NAKAMOTO, M., TAMAKI, Y., SASAMA, T., SAKITA, I., NAKAJIMA, Y., MONDEN, M., TAMURA, S. Image guidance of breast cancer surgery using 3D ultrasound images and augmented reality visualization. *IEEE Transactions on Medical Imaging*, 1998, vol. 17, no. 5, p. 681 – 693.

About Authors...

Asterios ANAGNOSTOUDIS was born in Thessaloniki, Greece. He received the Ing. (M.Sc.) degree in 2001 from the Faculty of Electrical Engineering and Communication (FEEC) of the Brno University of Technology (BUT), Brno, Czech Republic. Presently he is a Ph.D student at the Department of Biomedical Engineering, FEEC, BUT, Brno, Czech Republic.

Jiří JAN, born 1941 in Brno (Czech Republic), MScEE (1963), PhD in radio electronics (Brno UT 1969), scientific degree I (Czech Academy of Sciences, Prague 1986), Full Professor of Electronics (1991). **Present orientation:** digital signal and image processing, including applications in biomedical engineering. **Publications:** over 200 papers in journals and at conferences, books: Digital Signal Filtering, Analysis and Restoration (IEE Publ. London, UK 2000), also in Czech (1997, 2002); Medical Image Processing, Reconstruction and Restoration (CRC, USA 2005, in print). **Recent international activities:** Associate Editor of IEEE - Trans. on Biomedical Engineering (1996-2001). EURASIP central European liaison, since 1994. Czech Society for Biomedical Engineering - National Board member, 1990-2002. Member of Editorial Board, EURASIP Journal of Applied Signal Processing since 2000. Founding member of Engineering Academy of the Czech Republic (since 1994). Chair of international programme committee of biennial conference EURASIP - BIOSIGNAL'xx (supported by EURASIP and IEEE-EMBS). **Present position:** Head, Dept. of Biomedical Engineering and Coordinator of the Institute for Signal and Image Processing (ISIP), both of FEEC, Brno UT.

RADIOENGINEERING REVIEWERS

June 2005, Volume 14, Number 2

- FRÝZA, T., Brno University of Technology, Brno
- KRATOCHVÍL, T., Brno Univ. of Technology, Brno
- LEONE, M., Siemens, Munich
- LEVICKÝ, D., Technical University of Košice
- MARCHEVSKÝ, S., Technical University of Košice
- MIKAS, F., Czech Technical University, Prague
- MOHR, F., Univ. of Applied Sciences, Pforzheim
- PATOČKA, M., Brno Univ. of Technology, Brno
- POKORNÝ, M., VŠB - Technical Univ. of Ostrava
- ROUBÍK, K., Czech Technical University, Prague
- SVAČINA, J, Brno University of Technology, Brno
- TAHA-AHMED, B., Univ. Politecnica de Madrid
- VOREL, P., Brno University of Technology, Brno
- VRBA, J., Czech Technical University, Prague